Adsorption (2013) 19:821–833
DOI 10.1007/s10450-013-9525-4

The role of the cation in the oxygen isotopic exchange in crystalline sulfate salt hydrates

S. Attia · L. Hevroni · A. Danon · D. Meyerstein · J. E. Koresh · Y. Finkelstein

Received: 12 December 2012 / Accepted: 18 February 2013 / Published online: 3 March 2013

Abstract The oxygen isotopic exchange during dehydration and decomposition of five sulfate salt hydrates ($CoSO_4 \cdot 6H_2O$, $NiSO_4 \cdot 7H_2O$, $ZnSO_4 \cdot 7H_2O$, $CaSO_4 \cdot 2H_2O$, $Li_2SO_4 \cdot H_2O$) was studied in detail by temperature programmed desorption mass spectrometry (TPD-MS) in a supersonic molecular beam (SMB) inlet mode. Crystals of the ^{18}O-enriched salts were grown and the detailed desorption steps of the various gaseous products released during dehydration and decomposition of these compounds were recorded. The desorption patterns confirmed the known characteristic stepwise dehydration of these salts, where regardless of the crystalline structure and composition, in all the salts (excluding the Li and Ca sulfates) a major group of $n - 1$ loosely bounded water of crystallization molecules (out of total of n molecules in the fully hydrated form) are released at adjacent temperatures in a typical low temperature range (<200 °C), while the last, most strongly bounded water molecule, consistently desorbs at relatively higher temperatures ($240 < T < 440$ °C). Interestingly, it is established that the oxygen isotopic exchange occurs exclusively between that latter, most strongly bound water molecule, and the salt anion. Remarkably, the results point out that the exchange process is mostly of solid-solid nature. Finally, the results point out that the probability of the isotopic exchange increases with the increment in the desorption temperature of the last dehydration step, i.e. with the bond strength in the monohydrate, between the last water molecule of crystallization and the cation.

Keywords Temperature programmed desorption · ^{18}O · Isotopic exchange · Water of crystallization · Sulfate hydrate

1 Introduction

Dehydration of crystalline hydrates represents an important group of heterogeneous reactions (Galwey 2000). Although numerous studies of solid-state dehydration and decomposition have been published (Young 1966; Makatun and Shchegrov 1972; Lyakhov et al. 1974; Brown 1980; Galwey et al. 1981; Galwey 1985, 1992; Galwey and Mohamed 1987; Galwey and Laverty 1990; Tanaka et al. 1995; Brown et al. 1997; Koga and Tanaka 2002; Galwey and Brown 1999), the detailed mechanism of these reactions has still not been resolved. The dehydration reaction may comprise more than one type of chemical change, governed by the nature of the water in the crystal. While some of the water molecules are coordinated to the cation, others are associated to the anion via hydrogen bonds. In the former case, the reactant structure is maintained, or at most, undergoes minor structural modifications (Galwey 2000; Flanagan and Franklin 1971; Franklin and Flanagan 1972). In the second type however, the reactant structure is destabilized by the removal of constituent hydrogen bonded water molecules, and dehydration is accompanied with

S. Attia · L. Hevroni · A. Danon · J. E. Koresh · Y. Finkelstein (✉)
Chemical Division, Atomic Energy Commission, Nuclear Research Center of the Negev (NRCN), P.O. Box 9001, 84190 Beer-Sheva, Israel
e-mail: jacobf@nrcn.org.il

S. Attia · D. Meyerstein
Chemistry Department, Ben-Gurion University of the Negev, P.O. Box 9001, 84105 Beer-Sheva, Israel

D. Meyerstein
Biological Chemistry Department, Ariel University of Samaria, 40700 Ariel, Israel

a considerable, up to major, structural change (Galwey 2000; Flanagan and Franklin 1971; Franklin and Flanagan 1972). In both cases the exact mechanism, as well as the chemical and structural changes during the elimination of water, is not well understood. A.K. Galwey adequately summarized this problem in a comprehensive review (Galwey 2000): "Compounds containing common, or comparable, chemical constituents often exhibit quite different kinetic behaviors, whereas some apparently dissimilar substances react in similar ways. It has thus been long appreciated that some characteristic features (reactivity, kinetics, etc.) of decomposition of solids cannot be obviously or qualitatively related to identities or properties of the reactants".

The TPD technique (Danon et al. 1997) is a powerful quantitative and qualitative tool for high resolution analysis of discrete dehydration steps of hydrated salts (Danon et al. 2005). Thus, the TPD technique enables the elucidation of key steps in the dehydration mechanism.

In most sulfates, out of n crystallization water molecules, $n-1$ are coordinated to the cation, whereas the last one is associated with the sulfate ion (Galwey 2000; Varghese and Maslen 1985). On heating, the inorganic salt splits of its water molecules via sequential key reaction steps that occur along a respective characteristic temperature range. Depending on the heating rate, the coordinated water molecules are released up to 240 °C, whereas the remaining SO_4^{2-} associated one, and the most strongly bonded, is released above 250 °C. Upon further heating, above 600 °C, the dehydrated sulfate salt decomposes, releasing gaseous SO_2 and O_2 products. These fully resolved desorption steps of water molecules and decomposition products, make hydrated sulfate salts ideal complexes for gas evaluation studies throughout their dehydration and thermal decomposition processes.

The occurrence of oxygen isotopic exchange between the water of crystallization and the sulfate anion, during the dehydration of copper sulfate penta-hydrate, was recently demonstrated (Danon et al. 2005). The principal findings of Danon et al. (2005) were: (i) an occurrence of oxygen isotopic exchange between the water of crystallization and the sulfate ion was established (ii) the exchange was shown to occur specifically between the last, most strongly bounded, water molecule of crystallization and, at most, one oxygen atom in SO_4^{2-} (iii) the exchange occurs in the solid phase within the $CuSO_4$ crystalline salt. It was speculated (Danon et al. 2005) that the exchange is enabled during the re-phasing of the crystal, where desorption of the last water molecule causes the crystal to undergo a morphological change. This speculation relied on the fact that removal of H_2O changes the stabilizing forces in the crystal, so that dehydration is usually accompanied by recrystallization to the more stable lattice of a lower hydrate and/or to fulfill the coordination requirements of the cation (Galwey 2000). All in all, the latter result was considered as a remarkable finding as it confronts the common conviction of the unfeasibility of oxygen isotopic exchange in sulfates under geothermic conditions (Hall and Alexander 1940; Miyoshi et al. 1984; Hoering and Kennedy 1957; Rankama 1963).

Following this finding, it seemed of interest to extend the TPD experiments to other sulfate hydrates, as well as to selenate (Hevroni and Danon 2010; Hevroni et al. 2009) and nitrate hydrated salts (to be published). The hydrated salts studied may be generally formulated as $M{\cdot}SO_4{\cdot}nH_2O$ (or more conveniently in a matrix representation of the form $SO_4\begin{pmatrix} n \\ M \end{pmatrix}$, with M the metal cation and n the number of water of crystallization molecules that compose the fully hydrated crystal respectively). Utilizing the above notation, the following hydrated sulfate salts were studied in the present work:

$$SO_4\begin{pmatrix} 1 & 2 & 6 & 7 & 7 \\ Li_2 & Ca & Co & Ni & Zn \end{pmatrix}$$

The results suggest some apparently common, broad and general features that affect the exchange process and shed light on the key steps that govern the isotopic oxygen exchange, and in a more general fashion, the overall dehydration mechanism of hydrated solids.

2 Experimental details

2.1 Crystal growth

Commercial salts were purchased from Merck ($NiSO_4{\cdot}7H_2O$-99 %, $CoSO_4{\cdot}6H_2O$-99 %, $ZnSO_4{\cdot}7H_2O$-99.5 %, $CaSO_4{\cdot}2H_2O$-99 %, $Li_2SO_4{\cdot}H_2O$-99 %). ^{18}O enriched water (Hyox18 LTD) was purchased from ROTEM industries-Israel. The oxygen isotopic abundance of the enriched raw liquid water was verified by electrolyzing ca. 0.5 ml of it, collecting the released gaseous O_2 and measuring its isotopic composition with a QMG 422 Balzers quadruple mass spectrometer (QMS). Due to the poor, $\Delta(m/z) = 1$, resolution power of the QMS, the isotopic abundance was determined under the approximation that the signal at $m/z = 34$ is contributed solely by ^{16}O–^{18}O, thus neglecting the contribution from $^{17}O_2$ as its content is expected to be extremely low. The resulting uncertainty introduced by this assumption is by far smaller than the overall experimental uncertainty, and is thus insignificant to the deduced isotopic composition. Different growth routes were utilized in order to obtain in advance controlled and localized isotopic composition of the oxygen in the molecular targets, i.e. water of crystallization molecules and/or salt anion.

Initially, as purchased hydrated sulfate salts were fully dehydrated by prolonged evacuation at 350 °C, after which the dehydrated crystals were left to cool down to room

temperature (RT) under active vacuum. The dried crystals were then promptly dissolved to yield saturated solution, in either natural (^{16}O) or ^{18}O enriched water. Actual enrichments are indicated for each salt in the results section. Dissolution procedure was carried out at ambient temperature under room atmosphere in case of utilizing natural water, and with no contact with the atmosphere in enriched water. Recrystallization was sequentially carried out following dissolution by slow evaporation of the water solvent at RT. Final weights of grown crystals were of the order of few grams. From each freshly grown crystal batch, a minute amount was sampled, grained and structurally characterized by means of XRD crystallography (only for the Co, Ni, Zn and Ca sulfates) provided with a Bragg–Brentano diffractometer and a Cu anode. The Kα line was filtered by means of graphite moderator. Further, indirect verification, was provided by the TPD spectra themselves, where the desorption patterns (desorption peak temperatures) were compared to published data (Kolitsch 2001; Ptasiewicz-Bak et al. 1998; Stadnicka et al. 1987; Angel and Finger 1988; Elerman 1988; Kellersohn 1992; El-Houte et al. 1989; Chichagov 1997; Siriwardane et al. 1999).

As the present study deals with an isotopic exchange phenomenon in the solid phase, it is important to address in advance the argument of possible oxygen exchange during the crystallization procedures, which may allegedly occur between the water in the solution and the sulfate salt anion. Such an exchange will not only undesirably alter the predesigned ^{18}O enrichment of the crystallization water molecules; it would imply that the exchange occurs in the liquid phase. If so, our principal claim of occurrence of an oxygen isotopic exchange in the solid phase would be highly questionable. Nonetheless, such an exchange is not probable during our practical crystallization periods at RT. The primary reason for this is that oxygen exchange between SO_4^{2-} and H_2O is extremely slow, taking $\sim 10^5$ years at RT (Hall and Alexander 1940; El-Houte et al. 1989; Siriwardane et al. 1999; Zeebe 2010). Furthermore, such a possibility may be also ruled out for elevated temperatures as shown by Loyd (1968), for isotopic exchange in geothermal water reservoirs. Loyd (1968) reports that the half-time of the oxygen exchange reaction between water molecules and sulfate ions, at 80 °C in the liquid phase, is ca. 120 years. Assuming first order reaction kinetics, a period of 5 years would be required for the completion of 3 % oxygen exchange at 80 °C. Moreover, by accounting for mass conservation considerations which account for all the ^{16}O and ^{18}O containing- species that participate in the exchange reaction, prior and after the exchange, one may confidently conclude that our crystallization process does not introduce such an exchange.

Finally, all grown natural and enriched hydrated crystals were weighed, grained and heated in a controllable rate inside the TPD reactor to release their water of crystallization molecules and to further thermally decompose. The oxygen isotopic composition of the thermally desorbed water molecules, SO_2 and O_2 decomposition products, were measured at the outlet of the TPD apparatus within isotopic resolutions, using the QMS apparatus.

2.2 TPD setup and measurements

A detailed description of the TPD-MS experimental setup was reported elsewhere (Danon et al. 1997, 2005). Here we just mention principle key features that enabled the performance of the present study. The apparatus is schematically illustrated in Fig. 1. It incorporates an atmospheric pressure TPD reactor provided with a supersonic molecular beam (SMB) inlet. Basically, TPD-MS with SMB inlet involves coupling of paired differentially pumped vacuum compartments, connected via a nozzle capillary. Under that configuration, it is practically possible to link between the high vacuum required for the normal operation of the mass spectrometer and the atmospheric pressure at the sample-containing TPD reactor. Transfer of the thermally desorbed species from the sample inside the TPD reactor to the MS chamber is achieved by 50 standard cc per minute (sccm) flow of inert UHP dry Helium carrier gas. To avoid possible adsorption/desorption reactions of the desorbed water molecules along their trajectory throughout the system, the inlet as well as all tubing down to the mass-spectrometer are constantly heated to 100 °C. The combination of the nozzle and skimmer components creates a SMB of the desorbed products and the carrier gas. This SMB flies through the system tubing, free of any collisions with the walls, then enters axially to the mass spectrometer ion source and is ionized therein. As the heating rate directly affects the resolution of the peaks in the TPD profiles, with low rates yielding higher resolutions, TPD data were first acquired during linear programmed ramping of sample temperature between RT and 900 °C, utilizing various predetermined heating rates between 2° and 30° C/min, in search for an optimal resolution of the desorption peaks. A heating rate of 10° C/min was found to be satisfactory in producing good resolution in reasonable running times, and was thus used for all data acquisitions in order to keep comparative conditions for all measured samples. It is worth mentioning in that respect that various heating rates may also be utilized for deducing activation energies of desorption. However, due to structural variances in the TPD profiles, caused by the occurrence of polymorphs (see further discussion in the text), such a procedure could yield erroneous activation energies and was therefore left out of the scope of the present study. The oxygen isotopic abundance of the thermally desorbed water molecules was determined by accounting for the ratios of the areas

occupied by the TPD curves along the characteristic temperature desorption range of interest. These areas were determined by integrating over the background subtracted TPD curves of interest. The deduced abundances where then used to evaluate the depletion/enrichment percentages quoted in the results section. It should be emphasized that enrichment/depletion trends are evaluated in the present study solely by accounting for the mass ratio 20/18 of $H_2^{18}O$ and $H_2^{16}O$, while ignoring the ^{17}O abundance, being 0.038 % and ca. 1 % in natural water and in the commercial enriched water respectively. In addition, the 0.15 % abundance of D_2O is also not accounted for. Finally, further considerations that are related to the accuracy of the current measurements are worth mentioning. In comparison to the $CuSO_4{\cdot}5H_2O$ TPD profiles, the TPD spectra currently measured for the other hydrated salts differ only in the number of peaks, resolution, relative intensities and locations. In addition, some peaks may possess multi component contributions. The signal at $m/z = 32$ for instance, contains contributions from $^{16}O_2$ from the decomposition of the sulfate anion, and $^{16}O_2$ and ^{32}S from the fragmentation of $^{32}S^{16}O_2$ in the ionizing chamber. The extent of fragmentations is a function of the ionization voltage in the QMS source, and has known fixed values. It is thus possible to correct for these artificial contributions of fragmentations. Likewise, additional corrections were carried out for all measurements by accounting for the effect of spatial mass discrimination in the molecular beam. These latter corrections, although minor, were nonetheless carried out before deducing the ^{18}O enrichment values. Finally, correcting for differences in the instrumental response (sensitivity) of the QMS to the different species, by utilizing a calibration procedure, was skipped since our analysis relies on calculating relative intensities of different oxygen-containing isotopic species of the same ions. After accounting for the signal/noise ratio, reproducibility of the TPD scans, choice of base line, theoretical consideration, fragmentations, mass discriminations and ignoring ^{17}O and D_2O abundances, the quoted values have satisfactory low relative uncertainties of less than 15 % (within two standard deviations).

Fig. 2 TPD patterns from natural hydrated salts Zn (**a**), Co (**b**) and Ni (**c**). *Left hand frames* desorbed H_2O, *right hand frames* O_2 and SO_2 decomposition products of SO_4^{2-}. On the H_2O frames, continuous lines $m/z = 18$, *dashed lines* $m/z = 20$. The $m/z = 20$ curves are multiplied by $1/0.002 = 500$, the ratio of $^{16}O/^{18}O$ natural abundances and are artificially biased for clarity. TPD were taken at 10 °C/min heating rate

The same overall measurements and interpretation procedures, described previously for the measurements of copper sulfate (Danon et al. 2005), were applied for nickel ($NiSO_4{\cdot}7H_2O$), cobalt ($CoSO_4{\cdot}6H_2O$), zinc ($ZnSO_4{\cdot}7H_2O$), calcium ($CaSO_4{\cdot}2H_2O$) and lithium ($Li_2SO_4{\cdot}H_2O$) sulfates.

3 Results and discussion

Figure 2 summarizes the desorption patterns of H_2O, O_2 and SO_2 (continuous lines) from natural hydrated salts of

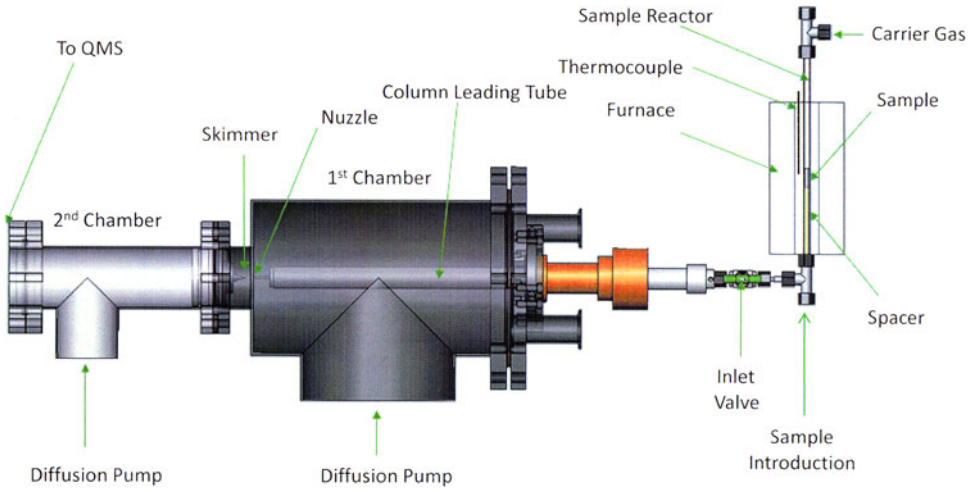

Fig. 1 Experimental setup of the TPD-MS-SMB apparatus. The TPD reactor (*right hand side*) is a 1/4″ tube located inside a cylindrical heater. The sample is placed at the *center* of the oven. Desorbed products are transported to the inlet by a carrier gas. The gas flows through a differential pump system composed of coupled paired differentially pumped vacuum compartments, connected via nozzle capillary. The combination of the nozzle and capillary components creates a supersonic molecular beam (SMB) of the desorbed products and the carrier gas. This SMB flies through the system tubing, free of any collisions with the walls, then enters axially to the mass spectrometer ion source and ionized therein

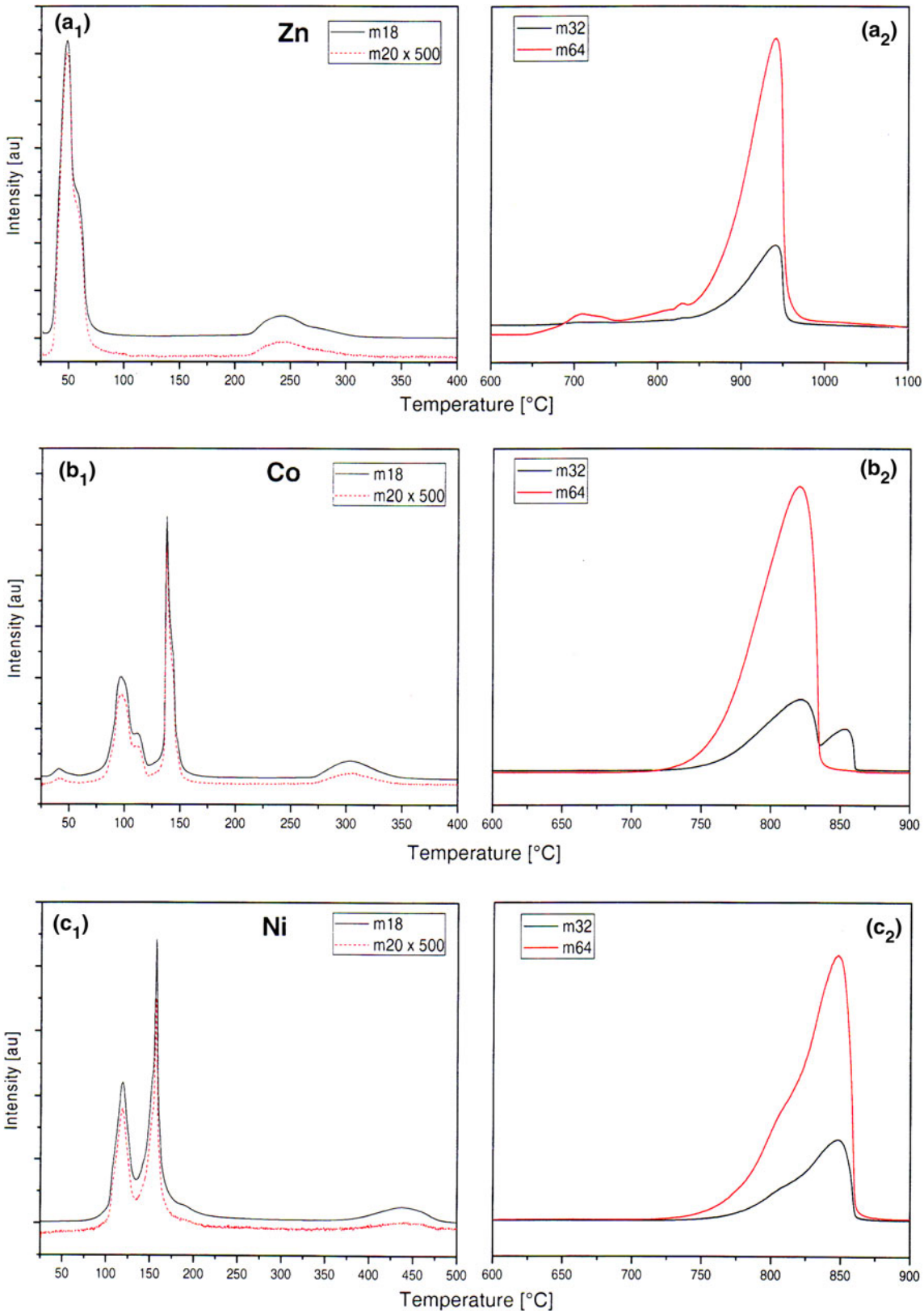

Zn (a), Co (b) and Ni (c). The dashed lines in the left hand frames of Fig. 2 depict the intensity of $m/z = 20$, the desorption curve of the enriched water molecules ($H_2^{18}O$). They are multiplied by a factor of ca. 500, the ratio of $^{16}O/^{18}O$ natural abundances (1/0.002), and are artificially biases downwards for clarity. It may be noted that in all

cases, the normalized $m/z = 20$ curves fully coincide those of $m/z = 18$, nicely illustrating the natural abundance of oxygen in the natural crystals.

3.1 Desorption and decomposition schemes of the hydrated sulfate salts

The TPD patterns of Fig. 2a all share a clear common behavior: whereas all $(n - 1)$ water of crystallization molecules desorb along the low temperature range, below 200 °C, leaving the crystalline salts in a monohydrate form, the last dehydration step, quantitatively involving the release of only one water molecule (by calibration), is peaked at significantly higher temperatures, above 240 °C. In addition, following the completion of dehydration, the sulfate anion in all these salts starts to decompose thermally above 600 °C. Shown on the right hand frames of Fig. 2 are the SO_4 thermal decomposition products, $^{32}S^{16}O_2$ ($m/z = 64$) and $^{16}O_2$ ($m/z = 32$), where $^{16}O_2$ is also contributed from the fermentation of SO_2 in the ion source. The above behavior, although satisfied by the Ni, Co and Zn sulfate salts, is not shared by the Ca and Li sulfates. These compounds will thus be discussed separately later on.

It should be noted that the rapid response time, <1 s (Danon et al. 1997), of the TPD apparatus is expressed in high resolution, which in turn may yield noticeable differences in the detailed fine structure of the desorption profiles, although acquired for a given salt. These differences can vary quite significantly according to the various parameters and experimental conditions that govern them, e.g. heating rate, carrier gas flow rate, crystal size etc. Nonetheless, the effect of such differences on the deduced relative enrichment of the desorbed species is practically insignificant because any quantification and enrichment determination have integrative character that relies on relative areas occupied under the measured profiles. Any dissimilarity between the fine structures of the TPD profiles taken for different crystals of the same salt, from either the same or different batches, is thus intrinsically hindered by accounting for the relative integrals/intensities of each crystal. All in all, with respect to data published in the literature (Kolitsch 2001; Ptasiewicz-Bak et al. 1998; Stadnicka et al. 1987; Angel and Finger 1988; Elerman 1988; Kellersohn 1992; El-Houte et al. 1989; Chichagov 1997; Siriwardane et al. 1999), where other experimental techniques were employed, a satisfactory agreement with the currently measured data is evident regarding the unambiguous occurrence of a separate, high T, desorption step that systematically involving the release of *one* last water molecule, i.e. that of the monohydrate form. Regarding the effect on the currently deduced enrichment values, as quantifications and enrichment determinations rely on the relative areas occupied under the measured TPD profiles of different isotopic forms of the same molecule/ion desorbed from a given crystal, e.g. between masses 20 ($H_2^{18}O$) and 18 ($H_2^{16}O$), any dissimilarities in the fine structure of desorption profiles between different crystals are intrinsically avoided when the degree of enrichment is derived.

The source of the differences between TPD profiles from crystals of the same growing batch might be due to the observation, at least for copper sulfate penta-hydrate, that water molecules in freshly as-grown crystals undergo continuous relocations between several effective lattice binding sites before the stable polymorphic form is obtained (Saig et al. 2003). In the case of $CuSO_4{\cdot}5H_2O$, this continuous kinetic process was shown to be accomplished within a period of ca. 1 week (Saig et al. 2003). Thus, the presently observed structure inconsistencies between different crystals of the same compound are attributed to either polymorphic effects and/or to the occurrence of surface effects due to the small dimensions of the crystals. In summary, whatever the source of differences between the shapes of the TPD profiles of these intermediate structures, they have an insignificant effect on the enrichment values deduced for each crystal.

Figure 2b$_1$ depicts the desorption profile of H_2O from $CoSO_4{\cdot}6H_2O$. It consists of a doublet desorption peak at 100 °C, followed by a rather sharp shouldered peak at 145 °C, and then a single shallow desorption peak at 315 °C. Accounting for crystal weight and the calibration curve, the water of crystallization content in the measured crystal is confirmed and the ratio (2.8:2.2:1) between the integrated areas of the above three TPD peaks suggest the following dehydration scheme:

$$CoSO_4 \cdot 6H_2O \rightarrow CoSO_4 \cdot 3H_2O + 3H_2O; \qquad 100\ ^\circ C \tag{1}$$

$$CoSO_4 \cdot 3H_2O \rightarrow CoSO_4 \cdot 1H_2O + 2H_2O; \qquad 145\ ^\circ C \tag{2}$$

$$CoSO_4 \cdot 1H_2O \rightarrow CoSO_4 + H_2O; \qquad 315\ ^\circ C \tag{3}$$

While the above desorption steps comply with published desorption temperatures, the stoichiometry is rather different than published in the literature (Straszko et al. 2000; Tomaszewicz and Kotfica 2003, 2004) where the first two dehydration steps were assigned to the release of two and three water molecules respectively. Here the order is reversed. Such a discrepancy may well be due to integration over tightly adjacent peaks. Nonetheless, the release of a single water molecule at 315 °C is in full accordance with the literature (Tomaszewicz and Kotfica 2003). As the temperature is further raised, the dehydrated salt starts to decompose at ca. 715 °C (Fig. 2b$_2$) according to the scheme:

$$3CoSO_4 \rightarrow Co_3O_4 + 3 \cdot SO_2 + O_2 \tag{4}$$

$$Co_3O_4 \rightarrow 3CoO + 1/2O_2 \tag{5}$$

The simultaneous occurrence of $m/z = 32$ (O_2/S) and 64 (SO_2) curves, peaked at about 820 °C, are due to the desorption of SO_3 which is then fragmented in the ion source of the mass spectrometer into SO_2 and $^1/_2O_2$. Following these peaks is a sole O_2 peak at 840 °C that is associated with decomposition of Co_3O_4. The above decomposition temperatures are lower by 60 °C from published data (Straszko et al. 2000; Tomaszewicz and Kotfica 2003).

Figures 2c$_1$, c$_2$ show the H_2O desorption and $NiSO_4$ decomposition respectively of $NiSO_4{\cdot}7H_2O$. Four H_2O desorption peaks may be noted; two unresolved peaks at 115 and 130 °C, one sharp split peak at 145 °C and then a single shallow desorption peak at 410 °C. In fact, some crystals exhibited an improved resolution between the first two adjacent peaks (not shown here). By accounting for the ratios between the integrated areas of the peaks in the higher resolved curves, we conclude the following dehydration scheme:

$$NiSO_4 \cdot 7H_2O \rightarrow NiSO_4 \cdot 5H_2O + 2H_2O; \quad 115\ ^\circ C \tag{6}$$

$$NiSO_4 \cdot 5H_2O \rightarrow NiSO_4 \cdot 3H_2O + 2H_2O; \quad 130\ ^\circ C \tag{7}$$

$$NiSO_4 \cdot 3H_2O \rightarrow NiSO_4 \cdot 1H_2O + 2H_2O; \quad 145\ ^\circ C \tag{8}$$

$$NiSO_4 \cdot 1H_2O \rightarrow NiSO_4 + H_2O; \quad 300\ ^\circ C \tag{9}$$

Here also, a discrepancy exists between the stoichiometry of dehydration steps along the low temperature range below 200 °C, but again, the last dehydration step at 300 °C is in full accordance with the literature (Siriwardane et al. 1999; Tomaszewicz and Kotfica 2004). As for the SO_4^{2-} decomposition (Fig. 2c$_2$), as for cobalt sulfate, simultaneous O_2 ($m/z = 32$) and SO_2 ($m/z = 64$) peaks are due to the desorption of SO_3 and its fragmentation in the ion source of the mass spectrometer. However, two differences are noted between the results in the nickel system and those in cobalt and copper (Danon et al. 2005) systems. (a) A shoulder is present at the low T wing of the peaks near 800 °C. This shoulder implies that $NiO{\cdot}NiSO_4$ may be a byproduct that then decomposes further to form nickel oxide. (b) The absence of a single O_2 desorption peak, implying that NiO is the decomposition product that as expected is not reduced further. These features are in accord with the decomposition pattern reported in the literature (Siriwardane et al. 1999; Tomaszewicz and Kotfica 2004). Thus the overall decomposition scheme of the dehydrated salt is:

$$NiSO_4 \rightarrow NiO(II) + SO_3(SO_3 \rightarrow SO_2 + 1/2O_2 \text{ in the ion source}) \tag{10}$$

In the desorption profile of $ZnSO_4{\cdot}7H_2O$ (Fig. 2a$_1$), two desorption peaks are evident; the first at 50 °C with a shoulder at ca. 60 °C, and the second at 240 °C. The relative areas occupied by the two peaks are 5.7:1, suggesting the following dehydration scheme:

$$ZnSO_4 \cdot 7H_2O \rightarrow ZnSO_4 \cdot 1H_2O + 6H_2O; \quad 55\ ^\circ C \tag{11}$$

$$ZnSO_4 \cdot 1H_2O \rightarrow ZnSO_4 + H_2O; \quad 240\ ^\circ C \tag{12}$$

The resolution in this case seems to be lower than that reported in the literature (Siriwardane et al. 1999), where two resolved peaks (three water molecule each) are observed in the low temperature range prior to the release of the seventh water molecule. The temperature range is however in accord with the published data. The SO_4^{2-} decomposition is initiated at ca. 650 °C (Fig. 2a$_2$). As in all the other salts studied here, gaseous SO_3 is released and further fragmented in the ion source of the mass spectrometer. Here again, the O_2 peak from the SO_3 fragmentation is not followed by a single O_2 desorption peak, implying that ZnO is the final product as expected, leading to the following decomposition scheme:

$$ZnSO_4 \rightarrow ZnO + SO_3(SO_3 \rightarrow SO_2 + 1/2O_2 \text{ in the ion source}) \tag{13}$$

In summary, the observed dehydration and decomposition patterns are in accord with the known characteristic stepwise dehydration of these salts, where regardless of crystalline structure and composition, a main group of $n - 1$ loosely bound water of crystallization molecules (out of total of n molecules in the fully hydrated form) are released at adjacent temperatures in a typical low temperature range (<200 °C), while in the remaining monohydrate, the last, most strongly bound water molecule, consistently desorbs at relatively higher temperatures ($240 < T < 440$ °C).

3.2 Isotopic exchange in the hydrated sulfate salts

The isotopic exchange processes of $NiSO_4{\cdot}6H_2O$, $CoSO_4{\cdot}7H_2O$ and $ZnSO_4{\cdot}7H_2O$ were studied, using the TPD-MS-SMB apparatus, and analyzed in an analogous procedure to that used for the $CuSO_4{\cdot}5H_2O$ system (Danon et al. 2005). Figure 3 summarizes the measured TPD profiles of the isotopic products from the Zn (a), Co (b) and Ni (c) hydrated sulfate salts grown in advance with the same ca. 50 % ^{18}O raw enriched water. As in Fig. 2, the left hand profiles are the low T regime, where the salts are dehydrated and the released water molecules are recorded, whereas the right hand ones depict the high T regime containing the SO_4^{2-} decomposition products.

Figure 3b$_1$ shows the desorption profiles of $H_2^{16}O$ ($m/z = 18$) and $H_2^{18}O$ ($m/z = 20$) over the course of dehydration of enriched $CoSO_4{\cdot}6H_2O$. The results clearly demonstrate that the isotopic composition of the first five water molecules of hydration, in analogy to the first four molecules released from $CuSO_4{\cdot}5H_2O$, have the same isotopic composition,

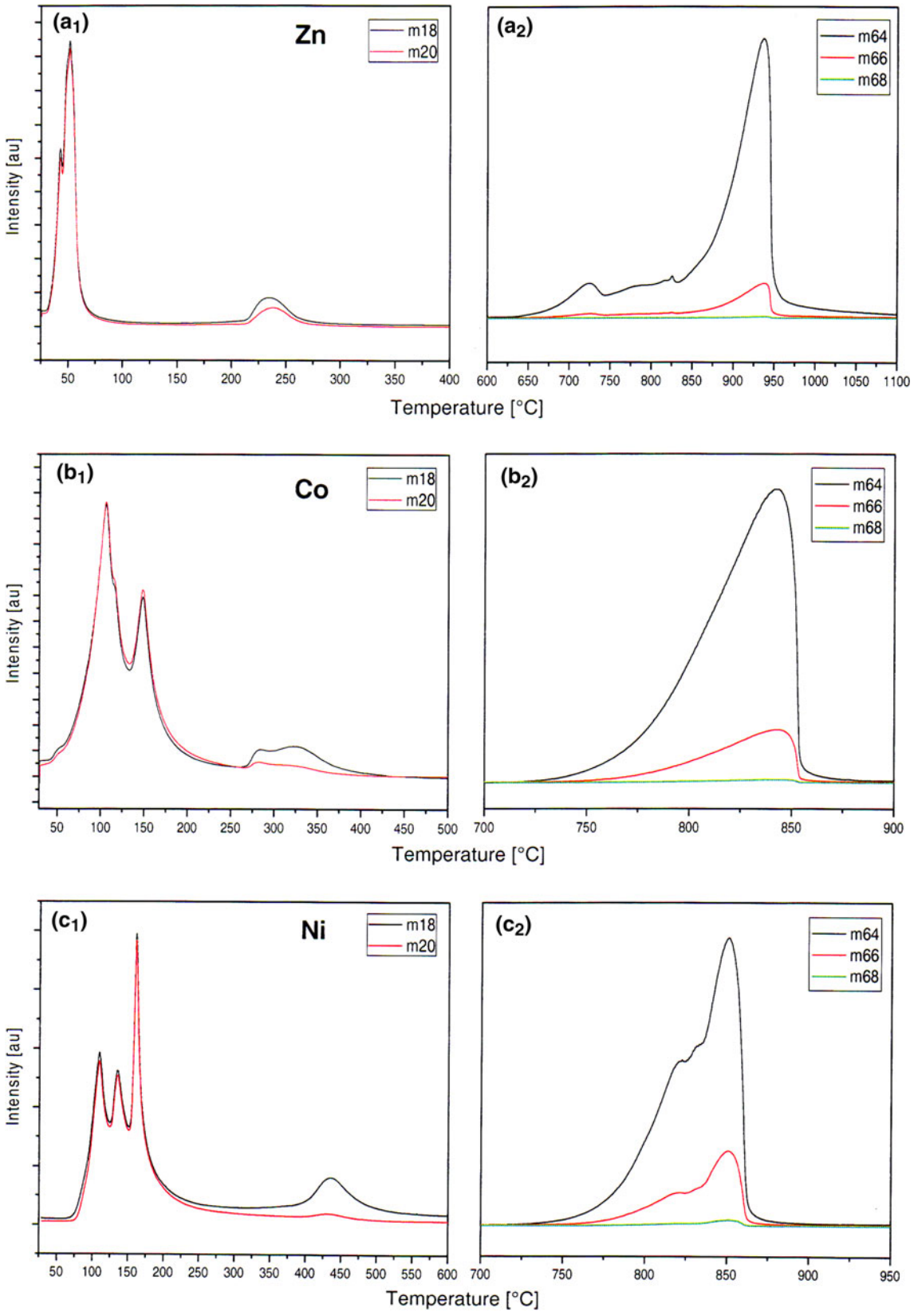
(a1)
Zn
m18
m20
(a2)
m64
m66
m68
Intensity [au]
Temperature [°C]
(b1)
Co
m18
m20
(b2)
m64
m66
m68
Intensity [au]
Temperature [°C]
(c1)
Ni
m18
m20
(c2)
m64
m66
m68
Intensity [au]
Temperature [°C]

◀ **Fig. 3** TPD patterns (10 °C/min) from ^{18}O enriched hydrated salts Zn (**a**), Co (**b**) and Ni (**c**). *Left hand frames* desorbed $H_2^{16}O$ ($m/z = 18$) and $H_2^{18}O$ ($m/z = 20$), *right hand frames* isotopic species of SO_2, the decomposition product of SO_4^{2-}: $m/z = 64$ ($^{32}S^{16}O_2$), 66 ($^{32}S^{16}O^{18}O + {}^{34}S^{16}O_2$) and 68 ($^{34}S^{16}O^{18}O + {}^{32}S^{18}O_2$). Intensity deficits are clearly noted for all salts in the last $m/z = 20$ $H_2^{18}O$ desorption peak, systematically accompanied with excess intensities at $m/z = 66$ and 68, indicating isotopic oxygen exchange between the last water of crystallization molecule and the sulfate anion

47.0 % ^{18}O, as that used in their crystallization. On the other hand, the isotopic composition of the last water molecule released, 26.5 % ^{18}O, is clearly considerably lower. The results presented in Fig 3b_2 demonstrate that the deficit in the $m/z = 20$ intensity in the third, the last water peak, is compensated by a significant increase in the intensity of $m/z = 66$ ($^{32}S^{16}O^{18}O + {}^{34}S^{16}O_2$). This clearly indicates that an isotopic exchange occurred between the sixth water of crystallization molecule and the sulfate anion. The quantitative analysis of the results, as discussed in detail in Danon et al. (2005), involves the areas of the peaks for $m/z = 64, 66, 68$ ($^{32}S^{18}O_2$) that have all contributions from the isotopic exchange. The $m/z = 70$ signal which corresponds to $^{34}S^{18}O_2$ was also measured; however its intensity was negligible and therefore discarded due to both the relative low natural abundances of ^{34}S (~4 %) and that of ^{18}O whose contribution to the intensity is determined by its square value. Also, the signal measured at $m/z = 66$ possess an apparent complexity as it involves contributions from various isotopic terms: $^{33}S^{16}O^{17}O$, $^{32}S^{17}O_2$, $^{34}S^{16}O_2$ and $^{32}S^{16}O^{18}O$. Nonetheless, while the first two terms may be ignored due to the low natural abundances of ^{33}S and ^{17}O, only a correction for the none-negligible but known natural abundance of ^{34}S is sufficient to correctly account for the net contribution from $^{32}S^{16}O^{18}O$ which is of our interest. The measured ^{18}O enrichment of the sulfate in the latter experiment amounts to 5.5 %. In order to confirm that the heavy oxygen in the sulfate anion indeed originates from the sixth, last water of crystallization molecule, the theoretical average enrichment of the salt prior to the exchange and the measured average enrichment after the exchange were calculated. If prior to the exchange, the natural ^{18}O abundance of the four oxygen atoms in the sulfate is 0.2 % and the ^{18}O enrichment of the six water of crystallization is 47.0 %, then the average ^{18}O enrichment of the hydrated salt prior to the exchange is $(6 \times 47.0 + 4 \times 0.2)/10 = 28.28$ %. Similarly, by accounting for the measured enrichments of the various TPD peaks of Fig. 3b_2, it can be shown that after the exchange the average ^{18}O enrichment is: $(5 \times 47.0 + 1 \times 26.5 + 4 \times 5.5)/10 = 28.35$ %. The enrichment in the SO_4^{2-} is deduced from the measurement of enrichment in the SO_2 fragment assuming that the enrichment of the SO_2 equals that of the SO_4^{2-} ion. The two averages are practically identical, pointing out that the isotopic exchange indeed occurs in the solid phase between the sixth water of crystallization molecule and the sulfate anion during the dehydration reaction in the TPD reactor.

Figure 3a and 3c show the isotopic TPD profiles of H_2O and SO_2 upon dehydration and decomposition of the $ZnSO_4 \cdot 7H_2O$ and $NiSO_4 \cdot 7H_2O$crystalline salts respectively. Examination of these profiles and calculating their integrated areas clearly points out the similarity to the $CoSO_4 \cdot 6H_2O$ system. Following the same methodology, ^{18}O enrichments prior and following the exchange were compared. The average enrichments prior/after the exchange were 27.4/27.6 % and 27.0/27.5 % for the Zn and Ni salts respectively.

In summary the results point out that during the dehydration of the $MSO_4 \cdot (H_2O)_n$ salts, M = Co; Ni; Cu (Danon et al. 2005) and Zn, an isotopic exchange occurs only between the last water of hydration and the sulfate anion in the solid phase. This similarity is striking as these salts have different crystallographic structures, dehydration and decomposition profiles.

It seemed of interest to study the analogous process in salts of main group cations that have fewer water molecules of crystallization. Calcium sulfate dihydrate, $CaSO_4 \cdot 2H_2O$, and lithium sulfate monohydrate, $Li_2SO_4 \cdot 1H_2O$, were chosen for this study. Presented in Fig. 4 are TPD profiles of water ($H_2^{16}O$-black and $H_2^{18}O$-red) released from $CaSO_4 \cdot 2H_2O$ grown from ca. 40 % ^{18}O enriched water. It is clearly noted that the TPD profile of Fig. 4 resembles an asymmetric broadened peak that is evident as a structural shoulder at its low temperature wing. Such a shoulder may stem from either a temperature overshoot or it may alternatively indicate the occurrence of overlapping adjacent dehydration peaks. A suspected overshoot is ruled out as the observed sample temperature (measured at close vicinity to the sample inside the TPD reactor) was fully in accord with the predetermined linear ramping temperature program of the TPD reactor. As for the possible existence of closely adjoining peaks, not only that the total integrated area of the TPD peak accords with a quantitative release of two water molecules (by calibration), as well as with XRD analysis which confirmed the $CaSO_4 \cdot 2H_2O$ structure, a multiple peak fitting procedure that was applied to the TPD profile resulted in two partially overlapping peaks (at 136 and 147 °C, not shown in Fig. 4), with an integrated areas ratio of 1:1.09. Within experimental uncertainties, the above fit may be viewed as strong evidence that $CaSO_4 \cdot 2H_2O$ gives up its two hydration water molecules in a rather simultaneous fashion. Worth mentioning are the discrepancies associated with the thermal dehydration of $CaSO_4 \cdot 2H_2O$; While some TGA measurements (Hall and Alexander 1940) suggest a two step dehydration path, in which 1.5 H_2O molecules are released at ~120 °C while the remaining hemi-hydrate looses 0.5 H_2O at ~160 °C, others (Salman and Khraishi 1988) propose a different route where desorption to the anhydrous phase occurs via a single step. Interestingly, Yamamoto and Kennedy (1969) showed that a

two step dehydration process (1.5 followed by 0.5 H_2O) may be realized in $CaSO_4{\cdot}2H_2O$ only at elevated pressures, between 4 and 30 kbar. In view of the above diversity, great care was presently taken in attempting to test and validate our observation of single step dehydration, and to rule out a resolution issue possibly occurring due to a fast heating rate. Initially, an additional TPD measurement was executed at a low heating rate of 2 °C/min and was found to reproduce the single asymmetric desorption peak similar to that presented in Fig. 4. Then, a series of TGA measurements with a very slow heating rate of 0.5 °C/min were preformed, which yet again resulted in a singlet. Finally, we carried out TGA isotherms at the dehydration temperatures (136 and 147 °C), with no particular indications of a two-step dehydration process. All together, the above set of measurements strongly supports the soundness of the conclusion that $CaSO_4{\cdot}2H_2O$ de-hydrates via a single step process, or via two partially overlapping processes. Lastly, in contrast to the other salts studied in the present work, no indications of isotopic exchange were observed during the dehydration of $CaSO_4{\cdot}2H_2^{18}O$, i.e. no deficit in the ^{18}O enrichment of the hydration water molecules was monitored. As dehydrated $CaSO_4$ decomposes only at about 1,100 °C (Salman and Khraishi 1988), far beyond the capabilities of our experimental setup, the isotopic composition of the sulfate was not analyzed. The TPD profile of water released from a 50 % ^{18}O enriched $Li_2SO_4{\cdot}H_2O$ is shown in Fig. 5. Clearly only single water desorption peak is observed. As in the calcium salt no oxygen isotopic exchange is observed.

It is of interest to note the temporal delay in the beginning of the $m/z = 20$ desorption peak in Figs. 4 and 5 (and in a less pronounced fashion also in the TPD spectra of all other salts). This delay is attributed to the kinetic

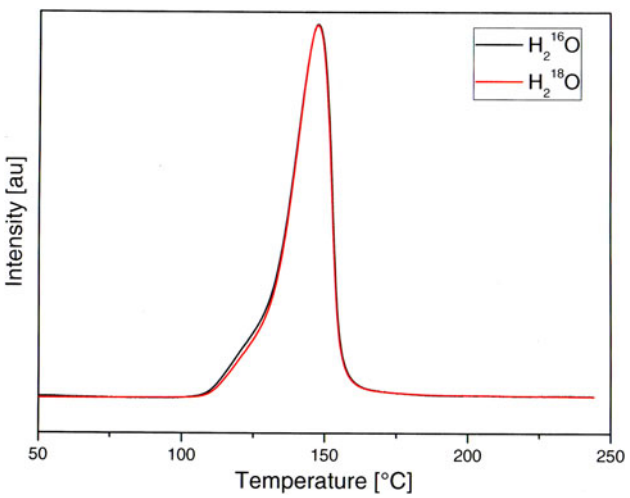

Fig. 4 TPD patterns of the isotopic species of water released from $CaSO_4{\cdot}2H_2O$. Crystals grown in water with ca. 40 % $H_2^{18}O$ enrichment. The $H_2^{18}O$ curve is normalized by a factor of 3/2, the ratio of $^{16}O/^{18}O$ abundances. TPD was taken at 10 °C/min heating rate

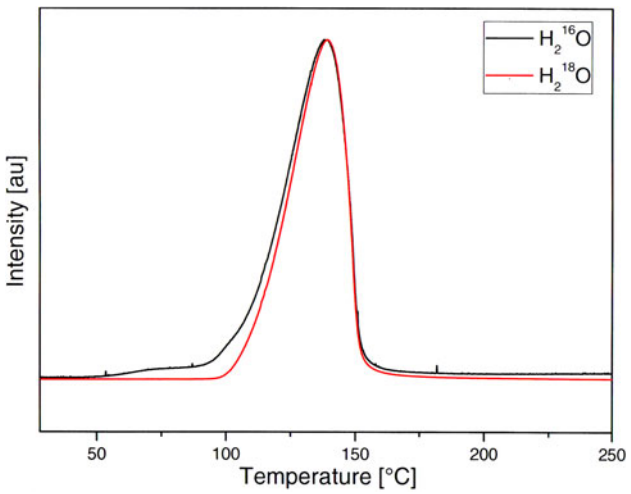

Fig. 5 TPD patterns of the isotopic species of water released from $Li_2SO_4{\cdot}H_2O$. Crystals grown in water with ca. 50 % $H_2^{18}O$ enrichment. TPD was taken at 10 °C/min heating rate

isotope effect, $H_2^{18}O/H_2^{16}O$, in the dehydration process. These differences further emphasize the high sensitivity of the present technique that enables observation of fine details in the TPD profiles.

3.2.1 *Isotopic exchange probability*

It is of interest to analyze the experimental data in terms of the probability P, of finding the ^{18}O atom of the last crystallization water molecule in the sulfate anion as a consequence of the atom exchange. This probability is expected to stay intact for a given salt, irrespective its initial ^{18}O enrichment. We hereby evaluate P by accounting for a simple, straightforward statistical model that is parameterized by the initial and final ^{18}O enrichments of the hydration water and of the sulfate anion. This evaluation may be tested by taking the parameters that were obtained experimentally for each salt as input data into the expression of P. Such a check can provide further insight into the role of the cation in the exchange process. P, the probability of the exchange, is calculated assuming that the exchange occurs between the oxygen atom of the last water molecule and the four oxygen atoms in SO_4^{2-}. Let $w_{(i)}$ and $s_{(i)}$ be the initial ^{18}O enrichments of the crystallization water molecules and of the sulfate anion respectively, prior to the exchange. The final enrichment of the last water molecule, $w_{(f)}$, may be expressed by $w_{(f)} = P \times s_{(i)} + (1 - P) \times w_{(i)}$, from which it follows that $P = \left(w_{(i)} - w_{(f)}\right)/\left(w_{(i)} - s_{(i)}\right)$. Alternatively, the average ^{18}O enrichment in the sulfate anion will be the sum of the following products: $P\ (w_{(i)} + 3 \times S_{(i)})/4$ and $(1 - P){\cdot}\ s_{(i)}$, whence: $P = 4(s_{(f)} - s_{(i)})/(w_{(i)} - s_{(i)})$, where $s_{(f)}$ is the deduced final enrichment of the sulfate anion. In order to test this model, great care was taken in providing identical

conditions for all salts, i.e. all the salt crystals were grown with the same enriched raw water. Furthermore, great care was taken to accurately deduce the values of $w_{(i)}, s_{(i)}$, $w_{(f)}$ and $s_{(f)}$. This was done by carefully correcting for both isotopic isobars originating from the sulfate isotopes as well as for the mass discrimination effects in the molecular beam due to mass differences of the various masses of ions flowing into the mass spectrometer. Then, the corrected $w_{(i)}, s_{(i)}$, $w_{(f)}$ and $s_{(f)}$ values were introduced in fractional form into the two equivalent formulas of P. The resulting P values are summarized in Table 1.

As expected the values of P nicely agree with the expected equivalency of the two P expressions. It is of interest to note that the exchange probability increases with the desorption temperature, T_d, of the last water of crystallization molecule. This observation might be attributed either to the stronger M–O bond, that polarizes the water molecule and increases the probability of oxygen atom exchange or to the higher temperature at which the process occurs that might provide the required activation energy. In that respect, tracing out and measuring a monohydrate salt which gives up its hydration water molecule below ca. 240 °C, can be of great interest. Possible candidates for such a check are: (i) $3CdSO_4{\cdot}8H_2O$ which dehydrates via two steps (Nobuaki 1993), $3CdSO_4{\cdot}8H_2O \rightarrow 3CdSO_4{\cdot}H_2O + 5{\cdot}H_2O$ at 131 °C and $CdSO_4{\cdot}H_2O \rightarrow CdSO_4 + H_2O$ at 223 °C (ii) $KMnPO_4{\cdot}H_2O$ which dehydrates in a single step process at $T < 300$ °C (Noisong and Danvirutai 2010).

A final discussion concerning the nature of the exchange mechanism is in place. A possibility exists that at elevated temperatures the released water molecules participate in the exchange, in their gaseous phase, with the solid anion. In order to test this issue, we have conducted the following set of experiments: dried natural $CuSO_4$ was kept at a predetermined temperature while being in contact with $H_2^{18}O$ vapor for 24 h, allowing it to undergo a possible oxygen isotopic exchange with the enriched vapor phase. The predetermined temperatures were chosen between 150 and 300 °C, so to cover the range of phases starting from the monohydrate and up to the fully dehydrated form of the salt. Following each dwelling time at each predetermined temperature, excess vapor was evacuated and the sample left to cool down to RT under the continuous flow of Helium carrier gas. A TPD measurement was then recorded up to high temperatures, exceeding the thermal decomposition of the sulfate anion. The resulting relative intensities of $S^{16}O_2$, $S^{16}O^{18}O$ and $S^{18}O_2$ (corrected for the natural abundance of ^{34}S) were such that could confirm the occurrence of only small extent of exchange. The results depicted the occurrence of a direct correlation between the dwelling temperature and the extent of isotopic exchange. Nonetheless, in all cases the resulting extent of exchange was consistently far less than that observed during the thermal dehydration of the hydrate salt. This result indicates that the exchange path is mainly of a solid–solid nature, with only a small solid–vapor fraction. It could also be the case that the last H_2O thermally dissociates and, within the crystalline bulk, its oxygen exchanges with an oxygen of the solid anion. On the other hand, it could well be the case that in the above experiment the surface area is insufficient to allow a large extent of vapor–solid exchange, while in the case of exchange during dehydration, the H_2O vapor stems from inside the crystal and is thus effectively exposed to a large surface area of the anion solid, increasing in turn the extent of exchange. Better insight into the fine details of the exchange mechanism may be gained by complementary studies utilizing in situ spectroscopic techniques such as IR and Raman that can be helpful in further description of the process.

4 Concluding remarks

The results obtained in this study can be summed up as follows:

In hydrated sulfate salts, oxygen atoms exchange between water of hydration and the sulfate anion in the solid state. This process was observed only for salts with more than one hydration molecule for which the dehydration path is such that a monohydrate is formed and dehydrates separately. Previous and ongoing studies indicate that this is also valid for the case of selenate (Hevroni and Danon 2010) and nitrate salts (to be published), in which

Table 1 The probability of oxygen isotope exchange between the last water of crystallization molecule and the sulfate anion for the various salts

Cation	T_d (°C)	$w_{(i)}$	$s_{(i)}$	$w_{(f)}$	$s_{(f)}$	$\frac{w_{(i)}-w_{(f)}}{W_{(i)}-S_{(i)}}$	$4 \times \frac{s_{(f)}-s_{(i)}}{W_{(i)}-S_{(i)}}$	P_{av}
Zn	240	0.43	0.002	0.313	0.036	0.273	0.318	0.296
Co	320	0.47	0.002	0.265	0.055	0.438	0.453	0.446
Ni	430	0.429	0.002	0.146	0.077	0.663	0.703	0.683

$w_{(i)}, s_{(i)}, w_{(f)}$ and $s_{(f)}$ are the actual measured initial (i) and final (f) ^{18}O fractional enrichments of the last water of crystallization molecule (w) and of the sulfate anion (s) respectively. The last three columns are the calculated Ps as explained in the text and their average value P_{av}. T_d is the measured desorption temperature of the last water molecule

the oxygen exchange occurs between water of hydration and the selenate/nitrate anion in its solid state.

This exchange occurs, at least for the cations studied, between the last water of hydration molecule, that of the monohydrate form, and the anion.

The probability of the atom exchange increases with the increase in the temperature at which the last water hydration molecule is lost.

This atom transfer was observed only for divalent transition metal sulfates and not for lithium and calcium salts. Whether this observation is due to involvement of d orbitals in the process or just to the weaker Lewis Acidity of the latter cations has to be checked in the future, e.g. by studying the dehydration of $Al_2(SO_4)_3{\cdot}9H_2O$.

The occurrence of isotopic exchange between water of hydration molecules and sulfate in the solid phase opposes the conventional hypothesis that oxygen exchange between minerals and their environmental surrounding is restricted to the liquid or gaseous phases. This result is of great significance regarding geothermic studies as it may have considerable implications on the determination of geothermic parameters. Nonetheless, complementary in situ spectroscopic IR and Raman studies are needed in order to achieve better insights into the fine details of the exchange mechanism and gain a more conclusive description of the process.

The results point out that the TPD-MS-SMB technique is sensitive enough to detect the $^{16}O/^{18}O$ kinetic isotope effect in the dehydration of $CaSO_4{\cdot}2H_2O$ and $Li_2SO_4{\cdot}H_2O$.

Overall, the fundamental properties and characteristic behaviors reported in the present study may be considered in general as potential classifying parameters in search for a unified formulation of solid-state dehydration reactions.

Acknowledgments We thank, N. Costirya, E. Harpenes, for technical assistance and Z. El-Maliach and E. Edri for water isotopic abundance measurements.

References

Angel, R.J., Finger, L.W.: Polymorphism of nickel sulfate hexahydrate. Acta Crystallogr. Sect. C **C44**, 1869–1873 (1988)

Brown, M.E.: Reactions in the Solid State. Elsevier, Amsterdam (1980)

Brown, M.E., Galwey, A.K., Guarini, G.G.T.: Structures and functions of reaction interfaces developed during solid-state dehydrations. J. Therm. Anal. **49**, 1135–1146 (1997)

Chichagov, A.V.: Crystallographic and crystallochemical database for mineral and structural analogues. http://database.iem.ac.ru/mincryst/index.php. Accessed Dec 1997

Danon, A., Avraham, I., Koresh, J.E.: Temperature programmed desorption-mass spectrometer with supersonic molecular beam inlet system. Rev. Sci. Instrum. **68**, 4359–4363 (1997)

Danon, A., Saig, A., Finkelstein, Y., Koresh, J.E.: A new route of oxygen isotope exchange in the solid phase: demonstration in $CuSO_4{\cdot}5H_2O$. J Phys. Chem. **B109**, 21197–21201 (2005)

Elerman, Y.: Refinement of the crystal structure of $CoSO_4{\cdot}6H_2O$. Acta Cryst. Sect. C **C44**, 599–601 (1988)

El-Houte, S., El-Sayed, A.M., Soerensen, O.T.: Dehydration of $CuSO_4{\cdot}5H_2O$ studied by conventional and advanced thermal analysis techniques. Thermochim. Acta **138**(1), 107–114 (1989)

Flanagan, T.B., Franklin, M.L.: Self-diffusion of water in uranyl nitrate hexahydrate. J. Phys. Chem. **75**, 1272–1278 (1971)

Franklin, M.L., Flanagan, T.B. (1972) Kinetics of dehydration of single crystals of uranyl nitrate hexahydrate. J. Chem. Soc. Dalton Trans. 192-196

Galwey, A.K.: Structure and order in thermal dehydrations of crystalline solids. Thermochim. Acta **355**, 181–238 (2000)

Galwey, A.K., Spinicci, R., Guarini, G.G.T.(1981) Nucleation and growth processes occurring during the dehydration of certain alums: the generation, the development and the function of the reaction interface. Proc. R. Soc. London, [Ser.] A 378, 477-505, 6 plates

Galwey, A.K., Brown, M.E.: Thermal Decomposition of Ionic Solids. Elsevier, Amsterdam (1999)

Galwey, A.K.: Some recent studies of the mechanisms of dehydration reactions of solids. J. Therm. Anal. **38**, 99–110 (1992)

Galwey, A.K.: Solid state decompositions: the interpretation of kinetic and microscopic data and the formulation of a reaction mechanism. Thermochim. Acta **96**, 259–273 (1985)

Galwey, A.K., Laverty, G.M.: The nucleus in solid state reactions: towards a definition. Solid State Ionics **38**, 155–162 (1990)

Galwey, A.K., Mohamed, M.A.: Structure and function of the nuclei developed during dehydration of the alums aluminum potassium sulfate dodecahydrate ($KAl(SO_4)_2{\cdot}12H_2O$) and chromium potassium sulfate dodecahydrate ($KCr(SO_4)_2{\cdot}12H_2O$). Thermochim. Acta **121**, 97–107 (1987)

Hall, N.F., Alexander, O.R.: Oxygen exchange between anions and water. J. Am. Chem. Soc. **62**, 3455–3462 (1940)

Hevroni, L., Danon, A.: Oxygen isotope exchange during thermal dehydration of copper selenate pentahydrate. Solid State Ionics **181**, 1565–1567 (2010)

Hevroni, L., Shamish, Z., Danon, A.: Thermal dehydration and decomposition of copper selenate pentahydrate. J. Therm. Anal. Calorim. **98**, 367–370 (2009)

Hoering, T.C., Kennedy, J.W.: The exchange of oxygen between sulfuric acid and water. J. Am. Chem. Soc. **79**, 56–60 (1957)

Kellersohn, T.: Structure of cobalt sulfate tetrahydrate. Acta Crystallogr. Sect. C **C48**, 776–779 (1992)

Koga, N., Tanaka, H.: A physico-geometric approach to the kinetics of solid-state reactions as exemplified by the thermal dehydration and decomposition of inorganic solids. Thermochim. Acta **388**, 41–61 (2002)

Kolitsch, U.: Copper(II) selenate pentahydrate, $CuSeO_4{\cdot}5H_2O$. Acta Crystallogr. Sect. E **E57**, i104–i105 (2001)

Loyd, R.M.: Oxygen isotope behavior in the sulfate-water system. J. Geophys. Res. **73**, 6099–6110 (1968)

Lyakhov, N.Z., Boldyrev, V.V., Isupov, V.P.: Role of physically adsorbed water in the mechanism of crystal hydrate dehydration. Kinet. Katal. **15**, 1224–1229 (1974)

Makatun, V.N., Shchegrov, L.N.: Form of water in inorganic crystal hydrates and features of their dehydration. Usp. Khim. **41**, 1937–1959 (1972)

Miyoshi, T., Sakai, H., Chiba, H.: Experimental study of sulfur isotope fractionation factors between sulfate and sulfide in high temperature melts. Geochem. J. **18**, 75–84 (1984)

Nobuaki, O.: Measuring crystal water in hydrates by thermogravimetry. http://www.siint.com/en/documents/technology/thermal_analysis/application_TA_063e.pdf. Accessed Mar 1993

Noisong, P., Danvirutai, C.: Kinetics and mechanism of thermal dehydration of $KMnPO_4{\cdot}H_2O$ in a nitrogen atmosphere. Ind. Eng. Chem. Res. **49**, 3146–3151 (2010)

Ptasiewicz-Bak, H., Olovsson, I., McIntyre, G.J.: Structure, charge and spin density in $Na_2Ni(CN)_4 \cdot 3H_2O$ at 295 and 30 K. Acta Crystallogr. Sect. B **B54**, 600–612 (1998)

Rankama, K.: Progress in isotope geology. In: Isotope Geology, pp. 705. Interscience, New-York (1963)

Saig, A., Danon, A., Finkelstein, Y., Kimmel, G., Koresh, J.E.: A continuous polymorphic transition of coordinating water molecules in $CuSO_4 \cdot 5H_2O$. J. Phys. Chem. Solids **64**, 701–706 (2003)

Salman, O.A., Khraishi, N.: Thermal decomposition of limestone and gypsum by solar energy. Sol. Energy **41**(4), 305–308 (1988)

Siriwardane, R.V., Poston Jr, J. A., Fisher, E.P., Shen, M., Miltz, A.L.: Decomposition of the sulfates of copper, iron(II), iron(III), nickel, and zinc: XPS, SEM, DRIFTS, XRD, and TGA study. Appl. Surf. Sci. **152**, 219–236 (1999)

Stadnicka, K., Glazer, A.M., Koralewski, M.: Structure, absolute configuration and optical activity of α-nickel sulfate hexahydrate. Acta Crystallogr. Sect. B **B43**, 319–325 (1987)

Straszko, J., Olszak-Humienik, M., Mozejko, J.: Study of the mechanism and kinetic parameters of the thermal decomposition of cobalt sulphate hexahydrate. J. Therm. Anal. Calorim. **59**, 935–942 (2000)

Tanaka, H., Koga, N., Galwey, A.K.: Thermal dehydration of crystalline hydrates: microscopic studies and introductory experiments to the kinetics of solid-state reactions. J. Chem. Educ. **72**, 251–256 (1995)

Tomaszewicz, E., Kotfica, M.: Mechanism and kinetics of thermal decomposition of nickel(II) sulfate(VI) hexahydrate. J. Therm. Anal. Calorim. **77**, 25–31 (2004)

Tomaszewicz, E., Kotfica, M.: Application of neural networks in analysis of thermal decomposition of $CoSO_4 \cdot 7H_2O$. J. Therm. Anal. Calorim. **74**, 583–588 (2003)

Varghese, J.N., Maslen, E.N.: Electron density in non-ideal metal complexes. I. Copper sulfate pentahydrate. Acta Crystallogr. Sect. B **B41**, 184–190 (1985)

Yamamoto, H., Kennedy, G.C.: Stability relations in the system $CaSO_4 \cdot H_2O$ at high temperatures and pressures. Am. J. Sci. Schairer **267A**, 550–557 (1969)

Young, D.A.: Decomposition of Solids. Pergamon, London (1966)

Zeebe, R.E.: A new value for the stable oxygen isotope fractionation between dissolved sulfate ion and water. Geochim. Cosmochim. Acta **74**, 818–828 (2010)